

Models of Wave Supported Clumps in Giant Molecular Clouds

R.F. Coker, J.G.L. Rae, and T.W. Hartquist

Department of Physics and Astronomy,
University of Leeds, Leeds LS2 9JT UK
email: robc@ast.leeds.ac.uk, jglr@ast.leeds.ac.uk, twh@ast.leeds.ac.uk

Received 2000; accepted 2000

Abstract. We present plane-parallel equilibrium models of molecular clumps that are supported by Alfvén waves damped by the linear process of ion-neutral friction. We used a WKB approximation to treat the inward propagation of waves and adopted a realistic ionization structure influenced by dissociation and ionization due to photons of external origin. The model clumps are larger and less centrally condensed than those obtained for an assumed ionization structure, used in some previous studies, that is more appropriate for dark regions.

Key words: ISM: magnetic fields – ISM: clouds – Turbulence – Waves

1. Introduction

Giant molecular cloud complexes (GMCs), the birth places of stars, are typically many tens of parsecs in linear extent and have masses from 10^4 to $10^6 M_\odot$ and temperatures of 10–30 K (see Hartquist et al. 1998 for a recent review). Observations of CO emission from GMCs (Blitz & Thaddeus 1980; Williams et al. 1995) show them to be composed of many smaller clumps that are a few parsecs in extent and contain $\lesssim 10^3 M_\odot$.

The widths of CO emission lines originating in individual clumps are supersonic and have been attributed to the presence of Alfvén waves having subAlfvénic velocity amplitudes (Arons & Max 1975). The Alfvén waves contribute to the support of a clump along the direction of the large-scale magnetic field; the damping of the waves affects the degree of support that they provide. An important and well understood mechanism for the damping of linear Alfvén waves in a partially ionized medium is that due to ion-neutral friction which depends on the ionization structure (Kulsrud & Pearce 1969). Ruffle et al. (1998, hereafter R98) and Hartquist et al. (1993) have emphasised that the dependence of the ionization structure on total visual extinction, A_V , should greatly influence the density profiles of clumps if Alfvén waves contribute

to their support. To quantify the assertion of Hartquist et al. (1993) and R98, we present in this paper models of plane-parallel, wave-supported GMC clumps like those identified in the work of Williams et al. (1995), who made a detailed analysis of the CO maps of the Rosette Molecular Cloud (RMC), identifying more than 70 clumps. The models that we have constructed are for RMC-type clumps in equilibrium, a restriction justified by the fact that clear spectral signatures of collapse have been found only when much smaller scale features have been resolved (see, e.g., Hartquist et al. 1998).

We have adopted a WKB description of the wave propagation as did Martin et al. (1997) in their work on wave-supported clumps. Their work differs substantially from ours in that they used an ionization structure appropriate for dark regions. Also, we have considered inwardly rather than outwardly propagating waves, as many of the clumps mapped by Williams et al. (1995) do not contain detected stars and may have no internal means of generating waves. Indeed, the waves may be produced at the surface of a clump by its interaction with an interclump medium.

Other authors have addressed the importance of photoabsorption for the effects that the ionization structure will have upon a clump’s dynamics. These authors have been concerned primarily with dense cores and/or envelopes around them; cores are much smaller-scale objects than the clumps identified in Williams et al. (1995). McKee (1989) addressed the possibility that collapse in a system of dense cores is a self-regulating process due to the ionization of metals such as Magnesium and Sodium by photons emitted by stars formed in the collapse; he was concerned with infall due to ambipolar diffusion of a large-scale magnetic field. Ciolek & Mouschovias (1995) have shown that the large-scale magnetic field can support a photoionized envelope around a dense core for a time that is very long compared to the ambipolar diffusion timescale in the center of the dense core. In contrast to McKee (1989) and Ciolek & Mouschovias (1995), Myers & Lazarian (1998) addressed the effect of photoabsorption on support by waves rather than by the large-scale

magnetic field. They stressed that observed infall of dense core envelopes is slower than that expected due to gravitational free-fall and more rapid than collapse due to the reduction by ambipolar diffusion of support by an ordered large-scale magnetic field. They considered collapse of material supported primarily by waves and subjected to an external radiation field. While they made clear comments about the importance of the A_V dependence of the ionization structure for their model, they did not perform any detailed calculations in which a realistic dependence of the ionization fraction on A_V was used.

Several sets of authors have considered nonlinear effects in the dissipation of waves supporting a clump. Gammie & Ostriker (1996) investigated models of plane-parallel clumps and from their “1 2/3-dimensional” models found dissipation times due to nonlinear effects to be longer than the Alfvén crossing times for a fairly large range of parameters. The three dimensional investigations of Mac Low et al. (1998) and Stone et al. (1998) suggest the more restrictive condition that the angular frequency of the longest waves be no more than a few times $2\pi/t_A$ (where t_A is the Alfvén crossing time) in order for the dissipation timescale due to nonlinear damping to be roughly the Alfvén crossing time or more. In most cases addressed in this paper we have restricted our attention to such angular frequencies so that we are justified to lowest order in focusing on only the damping due to ion-neutral friction. It should be noted that the above three dimensional studies of nonlinear effects concerned homogeneous turbulence and did not include ion-neutral damping for a realistic ionization structure. If we are correct in supposing that the waves in clumps are driven externally, then the turbulence is not homogeneous and its nature depends on both the viscous scale set by ion-neutral damping and the exact boundary conditions. The effects of nonlinear damping and multiple dimensions will be considered in subsequent work.

In Sect. 2 we present the equations for the wave energy, the static equilibrium clump structure, and the gravitational field. In Sect. 3 we give a description of the calculations of the ionization structure for various values of the clump density and A_V while Sect. 4 contains details of the models considered here. Finally, in Sect. 5, we present conclusions.

2. Equations of Wave Propagation and Static Equilibrium

We consider plane-parallel clumps with $z = 0$ corresponding to the clump midplane and $z = z_b$ (with z_b defined as positive) corresponding to boundary between the clump and the interclump medium. The large-scale magnetic field is taken to be $B_0\hat{z}$ with \hat{z} normal to the surface of a plane-parallel clump. We study waves of angular frequency ω propagating from $z = z_b$ in the $-\hat{z}$ direction.

The ion velocity can be expressed as

$$v_i = V e^{-i \int k_r dz}, \quad (1)$$

where V is defined below and k_r is the real component of the complex wave vector. Hartquist & Morfill (1984) used a two-fluid treatment to examine a related problem and showed that for an inwardly propagating linear Alfvén wave

$$\frac{d}{dz} (k_r v_i v_i^*) = \frac{V_2}{v_{A_i}^2} v_i v_i^*, \quad (2)$$

where v_i^* is the complex conjugate of the ion velocity perturbation and

$$V_2 \equiv \frac{\nu_0 \omega^3 \rho_n^2}{\nu_0^2 \rho_i^2 + \omega^2 \rho_n^2}, \quad (3)$$

where ρ_i is ion mass density and ρ_n is the neutral mass density. The ion Alfvén velocity is given by

$$v_{A_i}^2 = \frac{B_0^2}{4\pi \rho_i}. \quad (4)$$

The ion-neutral coupling frequency, $\nu_0 \rho_i$, is such that the momentum transfer per unit volume per unit time from ions to neutrals is given by $\nu_0 \rho_n \rho_i (v_i - v_n)$ where v_n is the velocity of the neutrals. To a reasonably good approximation, C^+ is the dominant ion and we may take

$$\nu_0 \rho_i \simeq 2.1 \times 10^{-9} \text{sec}^{-1} \left(\frac{n_i}{1 \text{ cm}^{-3}} \right) \quad (5)$$

where n_i is the ion number density (Osterbrock 1961). If the dominant ion species are very massive, as occurs at large A_V and densities, the constant would approach $2.3 \times 10^{-9} \text{s}^{-1}$. However, in this work we ignore this dependence and use $12 m_H$ as the mass per ion.

If V in Eq. 1 is written as $e^{\int k_i dz}$, where k_i is the imaginary component of the wave vector, and the linearized version of the induction equation (cf. Eq. 3 of Hartquist & Morfill 1984) is used, Eq. 2 yields

$$\frac{d}{dz} \left(\frac{k_r}{k_r^2 + k_i^2} b b^* \right) = \frac{V_2}{v_{A_i}^2} \frac{b b^*}{k_r^2 + k_i^2}, \quad (6)$$

where b is the perturbation magnetic field and b^* is its complex conjugate. In the WKB approximation, d^2V/dz^2 is taken to be equal to zero, which is equivalent to assuming

$$k_i^2 + dk_i/dz \ll k_r^2 \quad (7)$$

Then it follows (cf. Eq. 7b of Hartquist & Morfill 1984) that in the WKB approximation

$$k_r^2 \simeq \frac{\omega^2 + V_1}{v_{A_i}^2}, \quad (8)$$

with

$$V_1 \equiv \frac{\nu_0^2 \omega^2 \rho_n \rho_i}{\nu_0^2 \rho_i^2 + \omega^2 \rho_n^2}. \quad (9)$$

As is consistent with the WKB approximation, we assume $k_i^2 \ll k_r^2$ and substitute Eq. 8 into Eq. 6 to find

$$\frac{d}{dz} \left(\frac{v_{A_i} U}{\sqrt{\omega^2 + V_1}} \right) = \frac{V_2}{\omega^2 + V_1} U, \quad (10)$$

where $U = bb^*/16\pi$ is the time-averaged energy density of the perturbation magnetic field.

We solve Eq. 10 along with the static equilibrium equation

$$c_s^2 \frac{d(\rho_n + \rho_i)}{dz} + \frac{dU}{dz} = -(\rho_n + \rho_i)g \quad (11)$$

(Martin et al. 1997) and the gravitational equation

$$\frac{dg}{dz} = 4\pi G(\rho_n + \rho_i), \quad (12)$$

where c_s , g , and G are the isothermal sound speed, the strength of the gravitational field, and the gravitational constant, respectively.

We verify the assumption that $k_i^2 \ll k_r^2$ *a posteriori* by checking that

$$k_i = \frac{1}{V} \frac{dV}{dz} \simeq \frac{V_2}{v_{A_i} \sqrt{V_1}} \ll \frac{V_1}{v_{A_i}^2}. \quad (13)$$

Note that if Eq. 13 is satisfied, Eq. 7 is as well.

3. Calculations of the Ionization Structure

The ionization structure determined by R98 and presented in their Fig. 1 was calculated on the assumption that, due to shielding of the CO by itself and by H_2 , the rate of CO dissociation by photons of external origin is negligible. For a plane-parallel semi-infinite cloud with constant Hydrogen nucleus number density, $n_H = 10^3 \text{ cm}^{-3}$, we assume an A_V -dependent dissociation rate that results in a CO abundance relative to n_H , $x(\text{CO})$, that is in harmony with the measurements shown in Fig. 6 of van Dishoeck (1998). For the $n_H = 10^3 \text{ cm}^{-3}$ model, Table 1 gives $x(\text{CO})$ and the photodissociation rate as a function of A_V . Note that the total abundance of carbon nuclei relative to n_H is fixed at 10^{-4} . In the work reported here, we used an ionization fraction that depends on both A_V and n_H . Using the A_V -dependent CO photodissociation rate from Table 1, we calculated the fractional ionization as a function of A_V for $n_H = 3 \times 10^2, 3 \times 10^3$, and 10^4 cm^{-3} at various A_V values. A bilinear interpolation in A_V and n_H is used to find the actual ionization fraction used for a given point in the clump. For densities above 10^4 cm^{-3} we assume that the total ionization fraction, $\xi \equiv \rho_i/\rho_n$, goes as $n_H^{-1/2}$, as expected in a dark region. Note that in all models, A_V is always greater than 4 whenever $n_H > 10^4 \text{ cm}^{-3}$.

Since the depletions in RMC-type clumps are very uncertain, we present results for both depletion cases given in R98. As discussed therein (also see Shalabiea & Greenberg 1995), case A abundances resemble those seen in dark cores with $A_V \gtrsim 5$ while case B, with higher fractional abundances of lower ionization potential elements, is more appropriate for more diffuse clouds.

Table 1. Assumed CO Photodissociation Rates

A_V	Rate (sec^{-1})	$x(\text{CO})$
0.5	7.685×10^{-13}	9.132×10^{-7}
1.0	4.279×10^{-13}	2.248×10^{-6}
1.5	2.132×10^{-13}	5.248×10^{-6}
1.75	1.440×10^{-13}	7.538×10^{-6}
2.0	7.465×10^{-14}	1.226×10^{-5}
2.25	4.864×10^{-14}	1.503×10^{-5}
2.5	2.245×10^{-14}	2.166×10^{-5}
2.75	1.405×10^{-14}	2.381×10^{-5}
3.0	4.291×10^{-15}	3.621×10^{-5}
3.25	4.112×10^{-15}	3.620×10^{-5}
3.5	3.669×10^{-16}	6.336×10^{-5}
3.75	1.200×10^{-16}	8.976×10^{-5}
4.0	0	9.767×10^{-5}

4. Details of the Models

Many RMC-type clumps are not bound by their own gravity and must be confined by interclump media (Bertoldi & McKee 1992). We shall assume that an interclump medium is sufficiently tenuous that it does not shield the clump from the standard interstellar background radiation field used in the calculation of ξ so that $A_V = 0$ at $z = z_b$. The material on either side of the interface between a clump and the interclump medium is in two distinct phases, and we may assume that at its outer boundary a clump has a substantial density; we take $n(\text{H}_2) = n_H/2$ everywhere in the clump and at $z = z_b$ set $n(\text{H}_2) = n_b$. Waves may exist in the interclump medium and be partially transmitted into the clump, or, as mentioned earlier, may be generated near the interface by the interaction between the clump and the interclump medium. Consequently, we assume that the magnitude of the amplitude of the perturbation magnetic field, $\delta B = \sqrt{bb^*}$, is, at $z = z_b$, a substantial fraction, f_b , of the large-scale field, B_0 .

In all models we have taken the mean mass per neutral particle, μ_n , to be 2.3 amu, corresponding to 14% of the neutral particles being He and 86% being H_2 . As is consistent with data given by Savage & Mathis (1979), we have assumed

$$A_V = \frac{N_H}{1.9 \times 10^{21} \text{ cm}^{-2}}, \quad (14)$$

where N_H is the column density of Hydrogen nuclei. Also, the temperature throughout a clump was taken to be 20 K.

For a given setup, an initial boundary value of $g(z = z_b) \equiv g_b$, was selected and Eqs. 10, 11, and 12 were numerically integrated using an adaptive Gear algorithm (Gear 1971). The value of g_b was changed by iteration until the inner boundary condition $g(z = 0) = 0$ was satisfied. Note that as the total visual extinction (or, equivalently for a plane-parallel cloud, the column density) for a cloud is increased, the clump reaches a maximum size,

z_{\max} , and starts shrinking as a larger and larger thermal pressure (and therefore density) is required to balance gravity. Thus, as long as $z_b < z_{\max}$, there are two values of g_b for each setup that satisfy the boundary conditions. One solution has a relatively flat density profile and a small total visual extinction while the other solution is more centrally condensed. We deal here exclusively with the latter solutions.

We have considered other models but present full results only for models which have a total edge-to-center visual extinction of 5 magnitudes since, as discussed in R98, it is in the region of A_V of a few that clumps appear to begin to contain detected stars, while many dense cores may have $A_V \lesssim 5$ (McKee 1989). For our canonical model (Model 1) we require a velocity amplitude, V , of 2 km sec⁻¹ and an Alfvén speed, v_A , of 3 km sec⁻¹ at $A_V = 2$. Since the concentration of CO at $A_V \lesssim 2$ is very low and measurements of GMC clump CO profiles have a width of ~ 2 km sec⁻¹ (Williams et al. 1995), observations require such velocities to exist well within the cloud. Also, we use a wave frequency, ω , of 2×10^{-12} sec⁻¹; this results in relatively strong neutral-ion coupling while keeping the wavelength of the perturbing wave less than the size of the cloud. In other words,

$$\nu_0 \xi \ll \omega \lesssim \frac{2\pi}{\int dz/v_A}. \quad (15)$$

Within the above constraints, we find for our canonical model the solution requiring the smallest value of B_0 , and, since the velocity amplitude of a linear Alfvén wave is thought to be comparable to but less than the Alfvén speed, the largest value of f_b . However, throughout the clump, $V \leq v_A$, consistent with our assumption of linear Alfvén waves.

We present the results of 5 models. Model 1 is for the above canonical parameters with R98’s depletion case A while Model 2 is for case B. Model 3 is the same as Model 1 but with $\omega = 1 \times 10^{-12}$ to illustrate the effect of a scenario with roughly maximum ion-neutral coupling. Model 4 is as Model 1 but with an ionization profile given by $\xi = 3 \times 10^{-16} \rho_n^{-1/2}$ (see, e.g., McKee 1989 and Myers & Lazarian 1998). Thus, Model 4 is for a dark region surrounded by interclump material. Finally, for completeness, we present a model with no turbulence; Model 5 is identical to Model 1 except with $f_b = 0$. A summary of the parameters of the 5 models is given in Table 2. For all models, $n_b = 375$ H₂ cm⁻³ and $B_0 = 135$ μ G.

5. Results and Conclusions

In Fig. 1 we present density as a function of visual extinction for each of the 5 Models. It is clear that the newer ionization profiles used in Models 1–3 result in less condensed, more extended clumps than the profile used in Model 4. In fact, n_H is roughly proportional to $1/z$ in Models 1–3 while n_H goes roughly as $1/z^2$ in Model 4. In Fig. 2 we

Table 2. Summary of Parameters used in Models

Model	ω (sec ⁻¹)	f_b	z_b (pc)	Depletions
1	2×10^{-12}	0.436	0.455	A
2	2×10^{-12}	0.436	0.4855	B
3	1×10^{-12}	0.436	0.495	A
4 ^a	2×10^{-12}	0.436	0.1978	A
5	2×10^{-12}	0.0	0.082	A

^a Uses $\xi = 3 \times 10^{-16} \rho_n^{-1/2}$.

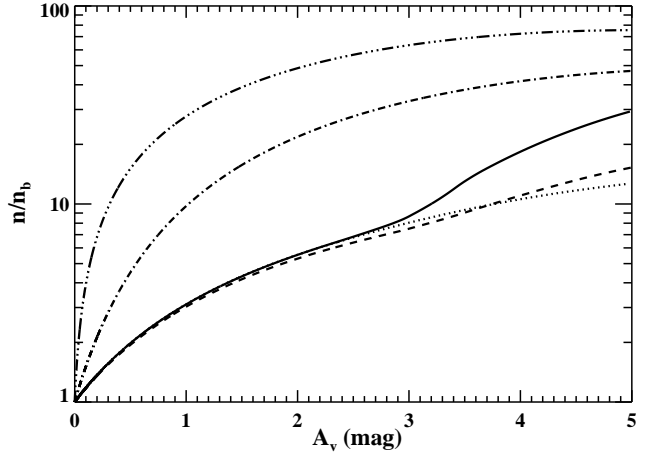


Fig. 1. Plot of density (normalized to the density at the outer edge of the clump) versus A_V for the 5 Models. The solid curve is for Model 1, the dotted curve for Model 2, the dashed curve for Model 3, the dot-dashed curve for Model 4, and the dash-chain-dot curve for Model 5.

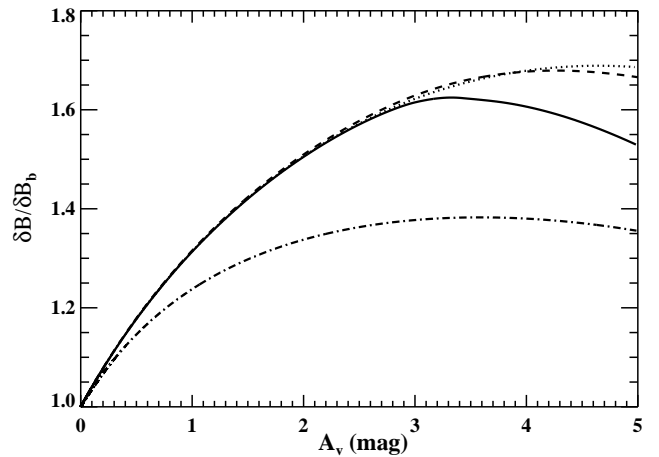


Fig. 2. As Fig. 1 but for the perturbing magnetic field, δB .

show plots of δB versus A_V for Models 1–4. Except for Model 4, which has k_i/k_r approaching 0.5 at the clump boundary so that Eq. 13 is not satisfactorily satisfied, the perturbing field obeys flux conservation near the surface of the clump. In Model 1, in the central region of the clump

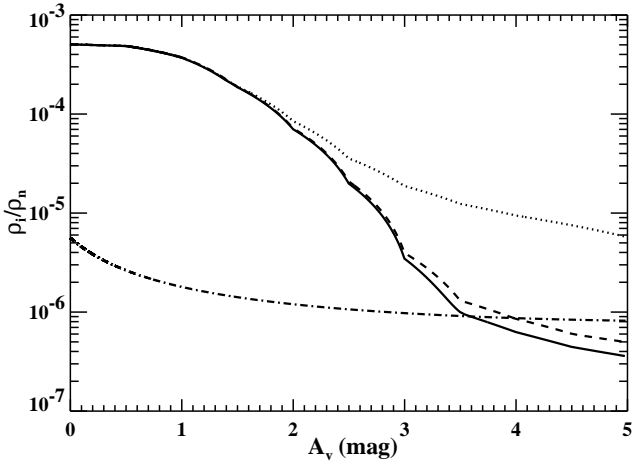


Fig. 3. As Fig. 1 but for the absolute ion mass fraction, ξ . The bumps seen on the curves for Models 1–3 are a result of the interpolation over A_V .

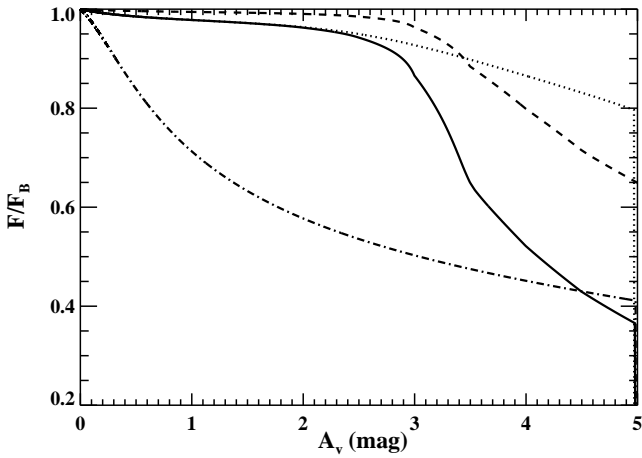


Fig. 4. As Fig. 1 but for the magnetic energy flux, $F \equiv k_T U \omega / |k|^2$.

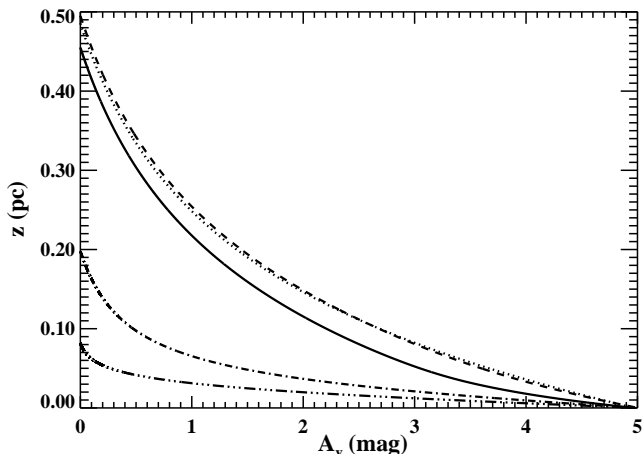


Fig. 5. As Fig. 1 but for z , the absolute spatial extent of the plane-parallel cloud.

dissipation is rapid enough that δB begins to decrease. In order to compensate for the loss of support, the equilibrium solution requires a complementary increase in the density, as can be seen in Fig. 1. On the other hand, in Model 4, the turbulence is dissipated much nearer to the cloud boundary, thus requiring a steeper overall density profile. The higher ionization fractions of the case B depletions result in very little dissipation even in the center of the clump for Model 2. Note that even though observations (Williams et al. 1995) suggest that the temperature of RMC-type clumps is closer to 10 K rather than the 20 K used here, thermal support is insignificant except in the centre of Model 1, so the effect of a lower temperature on the models would be merely to enhance slightly any central condensations.

The ionization profiles used in the Models are shown in Fig. 3. The ionization profiles described in Sec. 3 result in ξ for Models 1–3 being more than 50 times greater near the surface of the clump than in Model 4. However, in the center of the clump the ionization fraction drops, resulting in more dissipation. Again, this leads to clumps that are overall more diffuse but with small condensed cores. Clearly, clumps with $A_V \gtrsim 5$ will have distinct central condensations with $n/n_b \gtrsim 100$ and central fractional ionizations of $\lesssim 5 \times 10^{-7}$. Though dense cores may be formed during the fairly rapid collapse (as envisaged by Fielder & Mouschovias 1993) of more extended objects (i.e. RMC-like clumps) that become unstable, even in our equilibrium models we find central cores having densities and fractional ionizations similar to those measured for dense cores and their envelopes (Williams et al. 1995; Williams et al. 1998; Bergin et al. 1999).

Fig. 4 shows the flux of magnetic energy through the clumps for Models 1–4. Near the clump center, Model 1 is nearly thermally supported due to the dissipation of the turbulence. The higher ionization fraction for the case B depletions used in Model 2 results in less dissipation and thus more turbulent support for the clump. Consequently, as can be seen in Fig. 1, Model 2 has no central condensation and is more extended. Unfortunately, we can only speculate about how the depletions of Sulphur, metals, and some other species behave in RMC-like clumps (Ruffle et al. 1999). Thus, cases A and B are merely representative; as can be clearly seen in the figures, the clump profiles are very sensitive to the choice of abundances and the subsequent fractional ionizations. In addition, compared to Model 1, the stronger ion-neutral coupling in Model 3 results in less dissipation and subsequently the clump has little central condensation, as expected. Note however that for Model 3 the lower limit in Eq. 15 is not adequately satisfied.

Fig. 4 also shows the effect of external wave generation. If the fractional ionization is too low, as in Model 4, dissipation occurs close to the surface of the clump. Conversely, if the fractional ionization is too large, as in Model 2, significant dissipation occurs only at the clump's very

centre. Both extremes produce density profiles which lack a central condensation. Note that if our externally generated wave model is correct, one should not see turbulence within a condensed core if there is no turbulence in its surrounding envelope.

In Fig. 5 we present curves which map the visual extinction to the spatial extent of the clumps. Clouds with larger extents which match the observed 2–3 pc size of RMC-type clumps (Williams et al. 1995) cannot be reproduced within the constraints given in Sect. 4. However, observations generally measure the largest linear extent of a clump. Thus, since the waves only support the model clumps parallel to the large-scale field, it is not surprising that the model sizes given here are less than the observed sizes.

Similarly, the models require high boundary densities and magnetic field strengths in order for the Alfvén speed and wave velocity amplitude at visual extinctions where CO is abundant to be large enough to be compatible with observed linewidths. For Model 1, $n_b = 375 \text{ H}_2 \text{ cm}^{-3}$. This is rather higher than the typical value of $n(\text{H}_2) = 220 \text{ cm}^{-3}$ given by Williams et al. (1995) for RMC-type clumps but, given the uncertainties, it is within a reasonable range of the Williams et al. (1995) value. For Model 1, $B_0 = 135 \mu\text{G}$, significantly higher than the value of $30 \mu\text{G}$ suggested by observations (Heiles 1987) and expected from robust theoretical arguments (Mouschovias 1987). In order to determine whether the values of n_b and B_0 could be lower and still allow model properties to be consistent with observed linewidths, we constructed models for clumps with total edge-to-center extinctions of 3 magnitudes. The model giving $V = 2 \text{ km sec}^{-1}$ and $v_A = 3 \text{ km sec}^{-1}$ at $A_V = 2$ had $n_b = 325 \text{ H}_2 \text{ cm}^{-3}$, $B_0 = 105 \mu\text{G}$, $f_b = 0.49$, and $z_{\text{max}} = 0.565 \text{ pc}$; although n_b and B_0 were smaller and z_{max} larger, the agreement with observations is nonetheless poor.

Thus, the next step in the modelling of clumps in which wave support is important is the inclusion of wave support in models analogous to the axisymmetric models of magnetically and thermally supported clumps described in classic papers by Mouschovias (1976a, 1976b). It is possible that the inclusion of magnetic tension, as well as pressure, will allow the reduction of B_0 to a value more like that expected and the construction of models of clumps having larger linear extents.

References

Arons J., Max, C.E., 1975, *ApJ* 196, L77
 Bergin E.A., Plume R., Williams J.P., Myers P.C., 1999, *ApJ* 512, 724
 Bertoldi F., McKee C.F., 1992, *ApJ* 395, 140
 Blitz L., Thaddeus P., 1980, *ApJ* 241, 676
 Ciolek G. E., Mouschovias T.Ch., 1995, *ApJ* 454, 194
 Fiedler R. A., Mouschovias T.Ch., 1993, *ApJ* 415, 680
 Gammie C. F., Ostriker E. C., 1996, *ApJ* 466, 814

Gear C. W., 1971, Prentice-Hall Series in Automatic Computation, Prentice-Hall, Englewood Cliffs
 Hartquist T.W., Caselli P., Rawlings J.M.C., Ruffle D.P., Williams D.A., 1998. In: Hartquist T.W., Williams, D.A. (eds) *The Molecular Astrophysics of Stars and Galaxies*. Clarendon Press, Oxford, p. 101
 Hartquist T.W., Morfill G.E., 1984, *ApJ* 287, 194
 Hartquist T.W., Rawlings J.M.C., Williams D.A., Dalgarno A., 1993, *QJRAS* 34, 213
 Heiles C., 1987. In: Hollenbach D.J., Thronson, H.A. (eds) *Interstellar Processes*, Reidel, Dordrecht, p. 171
 Kulsrud R., Pearce W.P., 1969, *ApJ* 156, 445
 Mac Low M.-M., Klessen R.S., Burkert A., Smith M.D., 1998, *Physical Review Letters* 80, 2754
 Martin C.E., Heyvaerts J., Priest E.R., 1997, *A&A* 326, 1176
 McKee C.F., 1989, *ApJ* 345, 782
 Mouschovias T.Ch., 1976, *ApJ* 206, 753
 Mouschovias T.Ch., 1976, *ApJ* 207, 141
 Mouschovias T.Ch., 1987. In: Morfill G.E., Scholer M. (eds) *Physical Processes in Interstellar Clouds*, p. 453
 Myers P.C., Lazarian A., 1998, *ApJ* 507, L157
 Osterbrock D.E., 1961, *ApJ* 134, 270
 Ruffle D.P., Hartquist T.W., Caselli P., Williams D.A., 1999, *MNRAS* 306, 691
 Ruffle D.P., Hartquist T.W., Rawlings J.M.C., Williams D.A., 1998, *A&A* 334, 678 (R98)
 Savage B.D., Mathis J.S., 1979, *ARA&A* 17, 73
 Shalabiea O.M., Greenberg J.M., 1995, *A&A* 296, 779
 Stone J.M., Ostriker E.C., Gammie C.F., 1998, *ApJ* 508, L99
 van Dishoeck E.F., 1998. In: Hartquist T.W., Williams, D.A. (eds) *The Molecular Astrophysics of Stars and Galaxies*. Clarendon Press, Oxford, p. 53
 Williams J.P., Bergin E.A., Caselli P., Myers P.C., Plume R., 1998, *ApJ* 503, 689
 Williams J.P., Blitz L., Stark A.A., 1995, *ApJ* 451, 252